

〈Regular Article〉

Characterization of coronary calcified plaque by using multimodality intravascular imaging

Satoshi KOTO, Teruyoshi KUME, Takeshi NISHI
Hiroshi OKAMOTO, Ryotaro YAMADA, Terumasa KOYAMA
Tomoko TAMADA, Yoji NEISHI, Shiro UEMURA

Department of Cardiology, Kawasaki Medical School

ABSTRACT Background: This study aimed to evaluate the lipid contents of calcified plaques (CPs) and their clinical relevance to patients with coronary artery disease using near-infrared spectroscopy (NIRS) with intravascular ultrasound (IVUS) (NIRS-IVUS). Additionally, the morphological characteristics of lipid-containing CPs were assessed using optical coherence tomography (OCT).

Methods: This study was a retrospective observational study of consecutive patients who underwent both NIRS-IVUS and OCT. We identified CPs (calcification angle $> 45^\circ$) using grayscale IVUS and divided them into two groups (lipid group and no lipid group) based on the presence or absence of lipids using NIRS.

Results: Lipids were observed in 32 of 103 CPs (31%). During the per-patient analysis, patients with lipid-containing CPs had significantly higher serum total cholesterol levels than those without lipid-containing CPs ($p = 0.021$). Additionally, during the per-lesion analysis, it was observed that lipids accumulated more in the largest calcification arc of the CP and in adjacent segments in the lipid group than in the no lipid group (Region of interest: $p < 0.001$; proximal 4mm segment: $p = 0.002$; distal 4mm segment: $p = 0.013$). Lesions in the lipid group had more OCT characteristics representing plaque vulnerability, such as macrophages ($p < 0.001$) and layered plaques ($p < 0.001$), than those in the no lipid group. A multivariate logistic regression analysis revealed that only CPs with an unclear outer border, as assessed by OCT, were independent predictors of lipid contents within CPs ($p < 0.001$).

Conclusions: Multimodality imaging using NIRS-IVUS and OCT demonstrated that lipid-containing CPs were common in patients with high serum total cholesterol levels and could be identified by their outer borders during OCT imaging.

doi:10.11482/KMJ-E202349031 (Accepted on September 6, 2023)

Key words : Calcification, Coronary, Intravascular imaging

Corresponding author
Teruyoshi Kume
Department of Cardiology, Kawasaki Medical School,
577 Matsushima, Kurashiki, 701-0192, Japan

Phone : 81 86 462 1111
Fax : 81 86 464 1069
E-mail: tteru@med.kawasaki-m.ac.jp

INTRODUCTION

Coronary artery calcified plaques (CPs) not only imply the presence of coronary artery disease but also predict worse outcomes related to percutaneous coronary intervention (PCI)¹⁾. Our previous histological examination of CPs obtained from autopsy specimens demonstrated a variety of intraplaque tissue components, including a high incidence of lipid accumulation (necrotic tissue, 83%; fibrofatty tissue, 89%) within calcium deposits, which may be significant to their progression and clinical meanings²⁾. Among the various imaging modalities used to assess CPs, intravascular ultrasound (IVUS) is a widely used intracoronary imaging modality that enables direct visualization of the coronary arterial wall^{3, 4)}. IVUS is limited during the assessment of CP components because the bright signals from calcification cause saturation artifacts, thus making it difficult to assess neighboring tissue. Moreover, attenuation of the ultrasound beam by calcification causes acoustic shadowing, which impairs visualization of deeper vessel wall structures. Near-infrared spectroscopy (NIRS) with IVUS (NIRS-IVUS) is a recently developed spectroscopic method that

enables accurate evaluation of lipid contents within CPs. CPs with lipid contents, as demonstrated by NIRS, are sometimes observed during daily clinical practice. Therefore, this study aimed to evaluate the prevalence of lipid contents in CPs and their clinical relevance to patients with coronary artery disease. Additionally, the morphological characteristics of lipid-containing CPs were assessed using optical coherence tomography (OCT).

MATERIALS AND METHODS

Study population

This single-center, observational, retrospective study enrolled a total 62 consecutive patients who underwent both intracoronary NIRS-IVUS and OCT imaging of the native coronary arteries between January 2020 and May 2021. Among them, 6 patients were excluded from this study because they had acute myocardial infarction with thrombolysis in myocardial infarction flow grade 0 or 1 after thrombus aspiration or balloon angioplasty with a small balloon (diameter, ≤ 2.0 mm). Thirteen patients with poor-quality NIRS-IVUS or OCT images were also excluded. The patient inclusion and exclusion criteria are shown in Fig. 1. This

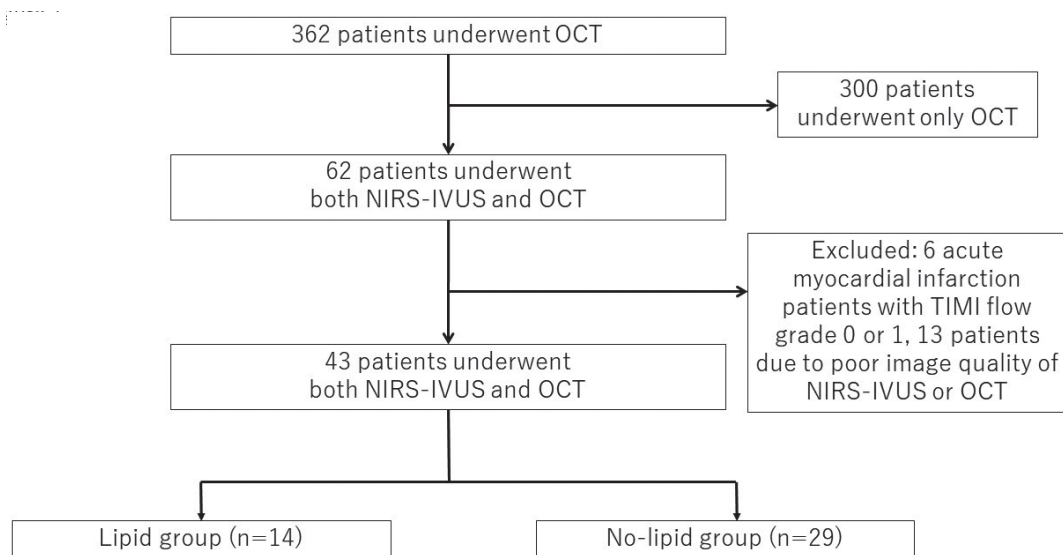


Fig 1. Flow diagram of patient inclusion and exclusion.

study was approved by the institutional review board of Kawasaki Medical School (IRB number: 5318-00) and conducted in accordance with the tenets of the Declaration of Helsinki regarding investigations involving humans.

Laboratory findings, including serum total cholesterol, high-density lipoprotein cholesterol, low-density lipoprotein cholesterol, HbA1c, and creatinine levels, were collected within 24 hours before performing coronary angiography or PCI.

NIRS-IVUS analysis

NIRS-IVUS hybrid imaging was performed using automatic pullback of the imaging catheter (Dualpro™ ; NIPRO, Tokyo, Japan) at 2.0 mm/sec and rotation of 1,800 rpm⁵⁾.

Among CPs exhibiting an area larger than 40%, those (calcification angle $> 45^\circ$) assessed using grayscale IVUS were selected, and lesions with the largest calcification angle were defined as regions of interest (ROIs). CPs were characterized by hyperechoic plaques that were brighter than the reference adventitia with shadowing on grayscale IVUS images⁶⁾. The Makoto® system (Infraredx; NIPRO, Tokyo, Japan) was used to analyze the chemogram data. Both analyses were conducted by independent cardiologists (A.K. and T.K.) who were blinded to the clinical and OCT characteristics of the patients. Using NIRS in the cross-sectional view, a high probability (> 0.6) of lipid plaques was displayed as yellow, and plaques without a prominent lipid core were displayed as red. The ROIs were divided into two groups based on the presence or absence of lipid contents (yellow color) within the CPs using NIRS (lipid group and no lipid group). To reveal the distribution of lipid contents in the CPs, their presence or absence was evaluated at each 1 mm up to 5 mm from the ROI. Using the longitudinal chemogram, the lipid contents were quantified as the lipid core burden index (LCBI), which was defined as the fraction of

valid pixels indicating lipids with a probability of > 0.6 within the scanned region multiplied by 1,000. The maximum LCBI at 4 mm (maxLCBI_{4mm}) was defined as the maximum LCBI value for any 4-mm region. A detailed description of NIRS-IVUS has been reported previously⁷⁾. The maxLCBI_{4mm} values 2 mm proximal to and 2 mm distal to (total of 4 mm) the ROI and in each of the proximal and distal 4-mm segments were compared between groups.

OCT analysis

OCT was performed using automatic pullback of the imaging catheter (ILUMIEN OPTIS or OPSTAR; Abbott Vascular, Santa Clara, CA, USA) at a speed of 36 mm/s, and an OCT analysis was performed using dedicated offline review systems. To compare the morphological characteristics of the CPs detected by NIRS-IVUS with the corresponding segments detected by OCT, ROIs were identified via landmark fiduciary points (e.g., side branches). Quantitative and qualitative OCT analyses were performed based on previously established criteria⁸⁻¹¹⁾. CPs were defined as regions of heterogeneous poor signals with clearly delineated contours. Additionally, the outer borders of the CPs were visualized using OCT. A qualitative assessment of characteristics representing plaque vulnerability, including macrophages, microchannels, layered plaques, and cholesterol crystals, was performed adjacent to (5 mm) and distal to the ROI. Macrophage infiltration was defined as a bright spot with high signal variance compared to the surrounding tissue¹²⁾. The microchannel was defined as tiny black holes (50-100 μm) within the plaque¹³⁾. Layered plaque was defined as a region with one or more layers with optical densities different from the underlying components and a clear border¹⁴⁾. Cholesterol crystals were defined as thin high-density linear regions without attenuation¹⁵⁾.

The OCT images were analyzed by 2 independent

OCT expert cardiologists (Koto S and Kume T). A consensus finding was obtained when there was concordance between the 2 independent OCT expert cardiologists. The interobserver reliability of the OCT qualitative findings, such as CP with non-clear outer border, macrophage, layered plaque, microchannel, and cholesterol crystals between the 2 OCT expert cardiologists was high (kappa coefficient = 0.87, 0.83, 0.91, 0.69, and 0.78, respectively).

Impacts of CP characteristics on change of troponin T following stent implantation

For selected patients with stable angina who underwent PCI, serum troponin T levels were measured before and the day after elective PCI. Changes in the serum troponin T levels (serum troponin T level the day after PCI and serum troponin T level on admission) of the lipid group and no lipid group were compared.

Statistical analysis

All analyses were performed using JMP version 14.2.0 software (SAS Institute, Cary, NC, USA).

Data are presented as means \pm standard deviations for continuous variables and as frequencies for categorical variables. A consensus finding was obtained when there was concordance between the 2 independent OCT expert cardiologists. The interobserver reliability of the OCT qualitative findings was analyzed by kappa statistic. Wilcoxon's rank sum test was used for continuous quantitative variables, and the Fisher's exact test was used to compare categorical variables. Variables with $p < 0.1$ in the univariate analysis were included in the multivariate logistic regression analysis to identify independent factors associated with lipid-containing CPs observed using NIRS. Significance was considered when $p < 0.05$.

RESULTS

Population and baseline clinical characteristics

A total of 43 patients was finally included in this study. The mean age was 70.6 (\pm 11.8) years, 79% were male. We successfully obtained multimodal images of 103 CPs (53 from left anterior descending coronary arteries, 16 from left circumflex coronary arteries, and 34 from right coronary arteries). Table

Table 1. Patient characteristics

	Lipid group (n = 14)	No-lipid group (n = 29)	P value
Age, y	70.9 \pm 12.5	70.2 \pm 11.5	0.857
Male	23 (79)	10 (71)	0.566
Admission diagnosis			
Stable angina	18 (62)	7 (50)	0.452
Unstable angina	4 (13)	2 (14)	0.965
Acute myocardial infarction	5 (17)	3 (21)	0.740
Others	2 (6)	2 (14)	
History of percutaneous coronary intervention	10 (34)	7 (50)	0.329
History of coronary artery bypass grafting	1 (3)	0 (0)	0.482
Risk factors	12 (85)	22 (75)	0.456
Hypertension	12 (85)	22 (75)	0.456
Dyslipidemia	12 (85)	18 (62)	0.113
Diabetes mellitus	6 (42)	14 (48)	0.738
Hemodialysis	3 (21)	8 (27)	0.664
Medications			
Aspirin	6 (42)	20 (68)	0.100
Clopidogrel	4 (28)	13 (44)	0.306
Statin		19 (65)	0.594

Values are mean \pm SD or n (%)

1 lists the characteristics of the patients. During the per-patient analysis, the lipid contents of the CPs of 14 of 43 (32.6%) patients were observed. There were no significant differences in the mean age, sex, clinical diagnosis, or history of coronary artery disease of the patients in both groups ($p > 0.05$). Table 2 presents the laboratory findings. Serum total cholesterol levels of the lipid group were significantly higher than those of the no lipid group (177 ± 39 mg/dL vs. 146 ± 34 mg/dL, $p = 0.021$). Low-density lipoprotein cholesterol levels tended to be higher in the lipid group; however, the difference was not statistically significant (92 ± 33 mg/dL vs. 75 ± 28 mg/dL, $p = 0.123$). Creatinine levels (2.06 ± 2.41 mg/dL vs. 2.52 ± 3.02 mg/dL, $p = 0.620$)

and HbA1c levels (6.2 ± 0.9 % vs. 6.6 ± 1.3 %, $p = 0.300$) did not differ between groups.

Intravascular imaging findings

During the per-lesion analysis, NIRS found lipid contents in 32 of 103 (31%) CPs detected using grayscale IVUS. Among the CPs observed in the lipid group, 59% were located in the left anterior descending coronary artery, 15% were located in the left circumflex coronary artery, and 25% were located in the right coronary artery. Of the CPs observed in the no lipid group, 47% were located in the left anterior descending coronary artery, 15% were located in the left circumflex coronary artery, and 36% were located in the right coronary

Table 2. Laboratory findings

	Lipid group (n = 14)	No-lipid group (n = 29)	P value
Serum total cholesterol (mg/dl)	177 ± 39	146 ± 34	0.021
HDL-cholesterol (mg/dl)	48 ± 13	42 ± 11	0.130
LDL-cholesterol (mg/dl)	92 ± 33	75 ± 28	0.123
HbA1c (%)	6.2 ± 0.9	6.6 ± 1.3	0.300
Serum creatinine (mg/dL)	2.06 ± 2.41	2.52 ± 3.02	0.620
eGFR (mL/min/1.73m ²)	50.2 ± 26.9	53.3 ± 37.9	0.775

Values are mean \pm SD or n (%). HDL, high-density lipoprotein; LDL, low-density lipoprotein; HbA1c, hemoglobin A1c; eGFR, estimated glomerular filtration rate.

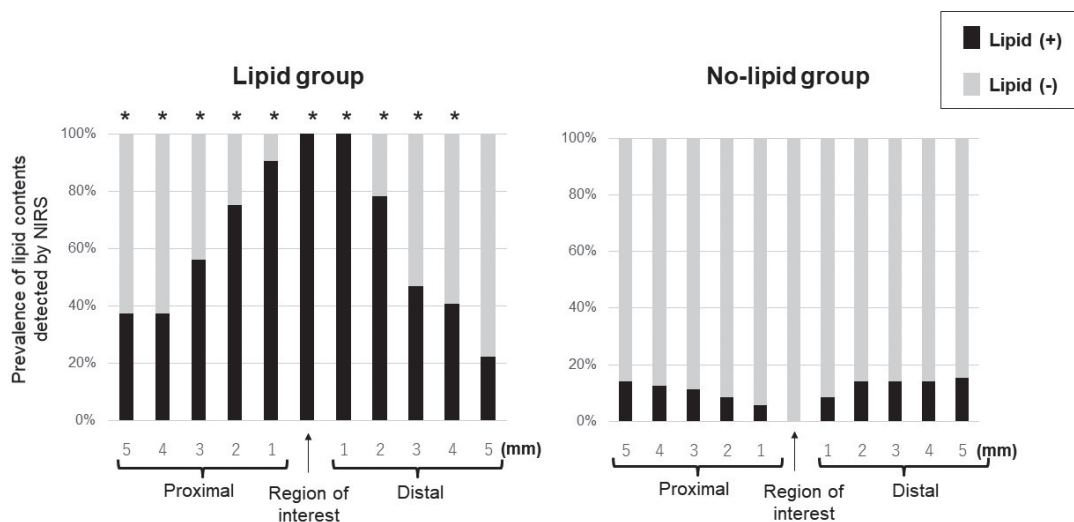


Fig 2. The distribution of lipid content at every 1 mm until 5 mm length from region of interest (ROI).

Prevalence of lipid contents detected by NIRS in the lipid-group was significantly higher not only in the ROI but also in the proximal 5 mm to distal 4 mm*. Lipid group vs. no-lipid group. P value < 0.05 .

artery. There was no significant difference in the CP distributions of the groups ($P = 0.479$). Fig. 2 shows the lipid content distribution around the ROI. The prevalence of the lipid contents detected by NIRS in the lipid group was significantly higher not only in the ROI (ROI: 100% vs. 0%, $p < 0.001$) but also in the 5-mm proximal (proximal 5 mm: 37% vs. 14%, $p = 0.007$; proximal 4 mm: 37% vs. 12%, $p = 0.003$; proximal 3 mm: 56% vs. 11%, $p < 0.001$; proximal 2 mm: 75% vs. 8%, $p < 0.001$; proximal 1 mm: 90% vs. 5%, $p < 0.001$) and 5-mm distal segments (distal 1 mm: 100% vs. 8%, $p < 0.001$; distal 2 mm: 78% vs. 14%, $p < 0.001$; distal 3 mm: 46% vs. 14%, $p < 0.001$; distal 4 mm: 40% vs. 14%, $p = 0.002$; distal 5 mm: 25% vs. 15%, $p = 0.249$). The maxLCBI_{4mm} values 2 mm proximal to and 2 mm distal to (total of 4 mm) the ROI and in each of the proximal and distal 4-mm segments were significantly higher in the lipid group than in the no lipid group (ROI: 340 ± 163 vs. 114 ± 139 , $p < 0.001$; proximal: 242 ± 179 vs. 112 ± 143 , $p = 0.002$; distal: 200 ± 172 vs. 122 ± 131 , $p = 0.013$) (Fig. 3). The OCT findings are presented in Table 3. The lumen area and largest calcification angle were not significantly different between groups ($p = 0.286$ and $p = 0.213$, respectively). In contrast, the OCT characteristics representing plaque vulnerability, such as macrophage infiltration and layered plaques, were observed more frequently in the lipid group than in the no lipid group ($p = 0.001$ and $p = 0.001$, respectively). Representative NIRS-

IVUS and OCT images are shown in Fig. 4. Using OCT, the prevalence of CPs with unclear outer borders was significantly higher in the lipid group than in the no lipid group (90% vs. 12%; $p < 0.001$). A multivariate logistic regression analysis was performed to identify predictors of CPs with lipid contents visualized by NIRS and found that only CPs with unclear outer borders assessed using OCT

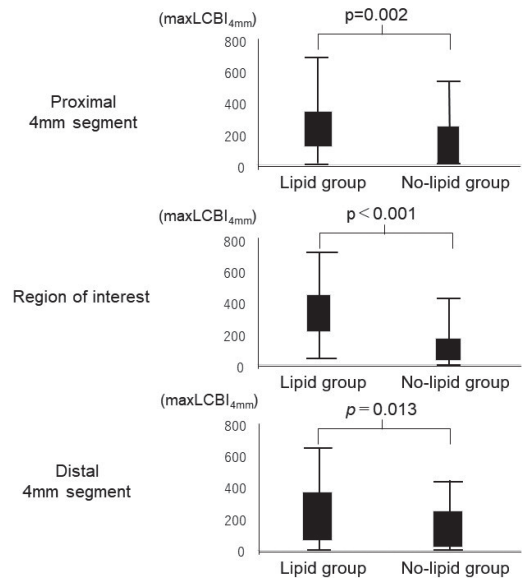


Fig 3. Box-whisker plots showing MaxLCBI_{4mm} values 2 mm proximal and distal to the ROI and in each of the proximal and distal 4 mm segments

The max lipid core burden index (LCBI)_{4mm} values 2 mm proximal and distal (total 4 mm) to the region of interest (ROI) and in each of the proximal and distal 4 mm segments were significantly higher in the lipid group than in the no-lipid group.

Table 3. Optical coherence tomography findings

	Lipid group (n = 32)	No-lipid group (n = 71)	P value
Lumen area (mm ²)	5.8 ± 0.5	6.6 ± 0.4	0.286
Largest calcification angle	214 ± 16	188 ± 12	0.213
CP with non-clear outer border	29 (90)	9 (12)	< .0001
Macrophage	22 (68)	24 (33)	0.001
Layered plaque	13 (40)	9 (12)	0.001
Microchannel	12 (37)	18 (25)	0.209
Cholesterol crystals	7 (21)	6 (8)	0.057

Values are mean ± SD or n (%). CP, calcified plaque.

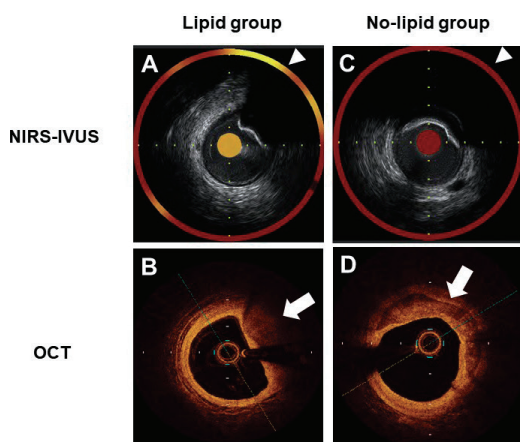


Fig 4. Representative NIRS-IVUS and OCT images of two types of calcified plaque

In the lipid group, gray-scale intravascular ultrasound (IVUS) shows hyperechoic findings with acoustic shadows recognized as calcified plaque (A). Near-infrared spectroscopy (NIRS) reveals lipid contents behind the calcification (A, arrowhead). Optical coherence tomography (OCT) imaging obtained at the same site shows calcification with a non-clear outer border, suggesting residual lipid contents within or near the calcification (B, arrow).

In the no-lipid group, gray-scale IVUS shows calcified plaque (C). NIRS demonstrates no lipid contents behind or near the calcification (C, arrowhead). OCT reveals calcification with a clear outer border, suggesting dense calcification filled with calcification (D, arrow).

were independent predictors of lipid contents within CPs visualized by NIRS (OCT: $p < 0.001$, odds ratio [OR] = 69.8, 95% confidence interval [CI] = 16.7-431.0; serum total cholesterol level: $p = 0.473$, OR = 0.99, 95% CI = 0.97-1.01; aspirin use: $p = 0.75$, OR = 1.25, 95% CI = 0.31-5.60; Macrophage: $p = 0.107$, OR = 3.2, 95% CI = 0.77-14.6; Layered plaque: $p = 0.651$, OR = 1.4, 95% CI = 0.30-6.4; Cholesterol crystals: $p = 0.388$, OR = 2.4, 95% CI = 0.64-26.1).

Impacts of CP characteristics on change of troponin T following stent implantation

Changes in the troponin T levels of 10 patients with stable angina before and after elective PCI were measured. In the lipid group ($n = 5$), the

change in the troponin T level tended to be higher than that in the no lipid group ($n = 5$); however, the difference was not statistically significant (0.11 ± 0.03 ng/mL vs. 0.09 ± 0.03 ng/mL, $p = 0.641$).

DISCUSSION

The main findings of the present study were as follows: lipid contents were observed in 32 of 103 (31%) CPs detected by grayscale IVUS; patients with lipid-containing CPs had significantly higher serum total cholesterol levels than those without lipid-containing CPs; lipids accumulated more in the largest calcification arc of the CP and adjacent segments in the lipid group than in the no lipid group; lesions in the lipid group had more OCT characteristics representing plaque vulnerability, such as macrophages and layered plaque, than those in the no lipid group; and CPs with lipid contents visualized by NIRS were characterized by OCT as CPs with unclear outer borders.

Our previous histological examination using autopsy specimens demonstrated a high incidence of hidden lipid contents within or near CPs *ex vivo*.² Consistent with these findings, during the present study, one-third of CPs evaluated with NIRS-IVUS exhibited lipid contents *in vivo*. Patients with lipid-containing CPs had characteristics that caused them to be at high risk for cardiovascular diseases, such as hypercholesterolemia. Although CPs, except for calcified nodules, are not thought to be vulnerable, the residual lipid contents of CPs might cause cardiac events and plaque progression. In fact, we previously reported a patient with acute coronary syndrome (ACS) caused by CP rupture demonstrated by NIRS-IVUS and OCT¹⁶. In such cases, residual lipid contents of CPs might cause ACS if the thin fibrous cap over the lipid contents is disrupted, even if surrounded by calcification. Additionally, heavily CPs are usually treated by using a debulking devices, such as rotational and orbital atherectomy¹⁷. If the calcification

surrounding lipid contents was debulked by rotational or orbital atherectomy, the residual lipid contents within CPs might contact with coronary blood flow and result in thrombus formation. This phenomenon might lead to the periprocedural myocardial injury indicating serum troponin T levels increase during PCI. During the present study, we compared the changes in serum troponin T levels of patients with stable angina before and after elective PCI. However, the changes in serum troponin T levels tended to be higher, but not significantly different, because the number of patients with serial troponin T measurements was limited (each $n = 5$). Furthermore, the finding that coronary segments with lipid-containing CPs are highly associated with characteristics of coronary plaque vulnerability, including macrophage infiltration and layered plaques, might indicate the possible future progression of coronary luminal stenosis and development of coronary events^{18, 19}. Further large-scale studies are required to verify the impact of lipid-containing CPs on short-term and long-term clinical outcomes.

A previous preliminary pathohistological study demonstrated a higher frequency of lipid contents in CPs with vague or invisible outer borders observed using OCT compared to those with clear outer borders²⁰. Consistent with these findings, the present study found a significantly higher prevalence of CPs with unclear outer borders assessed by OCT in the lipid group than in the no lipid group. Lipid contents are generally replaced by calcification from the outside over time, and those surrounded by calcification are generally recognized as CPs during OCT imaging because discrimination between lipid tissue and calcification is based on border characteristics (low intensity with diffuse border = lipidic tissue; low intensity with sharp border = calcification)^{8, 9}. Therefore, residual lipid contents within CPs could create problems during the evaluation of CPs using OCT, and it is necessary

to focus attention on the outer borders of CPs visualized using OCT in the clinical setting^{21, 22}.

LIMITATIONS

The present study had several important limitations. First, this was a single-center, retrospective observational study. Second, this study included a small number of patients. Third, consecutive patients who underwent both intracoronary NIRS-IVUS and OCT imaging were enrolled in this study. This may have led to selection bias.

CONCLUSIONS

Multimodality imaging including NIRS-IVUS and OCT demonstrated that CPs with high lipid contents were common in patients with high serum cholesterol levels and could be identified by their outer borders during OCT imaging.

ACKNOWLEDGMENTS

none

FUNDING

This research received no grants from any funding agency in the public, commercial, or not-for-profit sectors.

CONFLICT OF INTEREST

Teruyoshi Kume received remuneration from Abbott Vascular Japan. Shiro Uemura received remuneration from Abbott Vascular Japan, Daiichi-Sankyo, Novartis Pharma, Bayer, and Amgen and scholarship funds from Abbott Vascular Japan.

REFERENCES

- 1) Criqui MH, Denenberg JO, Ix JH, McClelland RL, Wassel CL, Rifkin DE, Carr JJ, Budoff MJ, Allison MA: Calcium density of coronary artery plaque and risk of incident cardiovascular events. *JAMA*. 2014; 311: 271-278.

- 2) Kume T, Okura H, Kawamoto T, *et al.*: Assessment of the histological characteristics of coronary arterial plaque with severe calcification.: *Circ J: official journal of the Japanese Circulation Society.* 2007; 71: 643-647.
- 3) Mintz GS, Nissen SE, Anderson WD, *et al.*: American college of cardiology clinical expert consensus document on standards for acquisition, measurement and reporting of intravascular ultrasound studies (ivus). A report of the american college of cardiology task force on clinical expert consensus documents. *J Am Coll Cardiol.* 2001; 37: 1478-1492.
- 4) Ikari Y, Saito S, Nakamura S, Shibata Y, Yamazaki S, Tanaka Y, Ako J, Yokoi H, Kobayashi Y, Kozuma K: Device indication for calcified coronary lesions based on coronary imaging findings. *Cardiovasc Intervent Ther.* 2023; 38: 163-165.
- 5) Kataoka Y, Puri R, Andrews J, Honda S, Nishihira K, Asami Y, Noguchi T, Yasuda S, Nicholls SJ: In vivo visualization of lipid coronary atheroma with intravascular near-infrared spectroscopy. *Expert Rev Cardiovasc Ther.* 2017; 15: 775-785.
- 6) Mintz GS: Intravascular imaging of coronary calcification and its clinical implications. *JACC. Cardiovasc Imaging.* 2015; 8: 461-471.
- 7) Kuku KO, Singh M, Ozaki Y, Dan K, Chezar-Azerrad C, Waksman R, Garcia-Garcia HM.: Near-infrared spectroscopy intravascular ultrasound imaging: State of the art. *Front Cardiovasc Med.* 2020; 7: 107.
- 8) Tearney GJ, Regar E, Akasaka T, *et al.*: Consensus standards for acquisition, measurement, and reporting of intravascular optical coherence tomography studies: A report from the international working group for intravascular optical coherence tomography standardization and validation. *J Am Coll Cardiol.* 2012; 59: 1058-1072.
- 9) Kume T, Akasaka T, Kawamoto T, Watanabe N, Toyota E, Neishi Y, Sukmawan R, Sadahira Y, Yoshida K: Assessment of coronary arterial plaque by optical coherence tomography. *The American journal of cardiology.* 2006; 97: 1172-1175.
- 10) Kume T, Okura H, Kawamoto T, *et al.*: Assessment of the coronary calcification by optical coherence tomography. *EuroIntervention : journal of EuroPCR in collaboration with the Working Group on Interventional Cardiology of the European Society of Cardiology.* 2011; 6: 768-772.
- 11) Fujii K, Kubo T, Otake H, Nakazawa G, Sonoda S, Hibi K, Shinke T, Kobayashi Y, Ikari Y, Akasaka T: Expert consensus statement for quantitative measurement and morphological assessment of optical coherence tomography: Update 2022. *Cardiovascular intervention and therapeutics.* 2022; 37: 248-254.
- 12) Tearney GJ, Yabushita H, Houser SL, Aretz HT, Jang IK, Schlerendorf KH, Kauffman CR, Shishkov M, Halpern EF, Bouma BE: Quantification of macrophage content in atherosclerotic plaques by optical coherence tomography. *Circulation.* 2003; 107: 113-119.
- 13) Kolodgie FD, Gold HK, Burke AP *et al.*: Intraplaque hemorrhage and progression of coronary atheroma. *N. Engl. J. Med.* 2003; 349: 2316-2325.
- 14) Okamoto H, Kume T, Yamada R, Koyama T, Tamada T, Imai K, Neishi Y, Uemura S.: Prevalence and clinical significance of layered plaque in patients with stable angina pectoris - evaluation with histopathology and optical coherence tomography. *Circ J: official journal of the Japanese Circulation Society.* 2019; 83: 2452-2459.
- 15) Nakamura S, Inami S, Murai K, Takano M, Takano H, Asai K, Yasutake M, Shimizu W, Mizuno K: Relationship between cholesterol crystals and culprit lesion characteristics in patients with stable coronary artery disease: An optical coherence tomography study. *Clinical research in cardiology : official journal of the German Cardiac Society.* 2014; 103: 1015-1021.
- 16) Sasahira Y, Kume T, Koto S, Hiroshi O, Yamada R, Neishi Y, Uemura S: Acute coronary syndrome demonstrating plaque rupture in calcified plaque visualized by optical coherence tomography and near-infrared spectroscopy combined with intravascular ultrasound. *Journal of cardiology cases.* 2021; 24: 193-194.
- 17) Ikari Y, Saito S, Nakamura S, Shibata Y, Yamazaki S, Tanaka Y, Ako J, Yokoi H, Kobayashi Y, Kozuma K: Device indication for calcified coronary lesions based on coronary imaging findings *Cardiovascular intervention and therapeutics.* 2023; 38: 163-165.
- 18) Usui E, Mintz GS, Lee T *et al.*: Prognostic impact of healed coronary plaque in non-culprit lesions assessed by optical coherence tomography. *Atherosclerosis.* 2020; 309: 1-7.
- 19) Araki M, Yonetsu T, Kurihara O *et al.*: Predictors of rapid plaque progression: An optical coherence tomography study. *JACC. Cardiovascular imaging.*

- 2021; 14: 1628-1638.
- 20) Ijichi T, Nakazawa G, Torii S, Nakano M, Yoshikawa A, Morino Y, Ikari Y: Evaluation of coronary arterial calcification - ex-vivo assessment by optical frequency domain imaging. *Atherosclerosis*. 2015; 243: 242-247.
- 21) Sonoda S, Hibi K, Okura H, Fujii K, Node K, Kobayashi Y, Honye J: Current clinical use of intravascular ultrasound imaging to guide percutaneous coronary interventions (update). *Cardiovascular intervention and therapeutics*. 2023; 38: 1-7.
- 22) Ozaki Y, Taniguchi M, Katayama Y, Satogami K, Ino Y, Tanaka A: Which is more useful for predicting no-reflow phenomenon? Insights from optical coherence tomography and coronary computed tomography. *Cardiovascular intervention and therapeutics*. 2023; 38: 246-247.